

# OPTICAL AND MICROPHYSICAL PROPERTIES OF AEROSOLS IN SOUTHERN (PEARL RIVER DELTA) AND NORTHERN CHINA (BEIJING) OBSERVED WITH RAMAN LIDAR AND SUN PHOTOMETER

Matthias Tesche, Detlef Müller, Ronny Engelmann, Dietrich Althausen, Ulla Wandinger, and Albert Ansmann

*Leibniz Institute for Tropospheric Research, Permoserstr. 15, D-04318 Leipzig, Germany,  
E-mail: tesche/detlef/ronny/dietrich/ulla/albert@tropos.de*

## ABSTRACT

Particle optical and microphysical properties, the vertical extent of the haze layer, and pronounced planetary-boundary-layer (PBL) developments in southern and northern China are presented. Results are based on vertically-integrated Sun photometer (SPM) and height-resolved Raman lidar observations. Measurements were conducted in subtropical Xinken (22.6°N, 113.6°E) near the southern coast of China and mid-latitude Beijing (39.9°N, 116.3°E), North China, in October 2004 and January 2005, respectively. Days of simultaneous measurements with lidar and SPM allowed us to apply a new approach [1] with our inversion scheme [2]. The solar aerosol radiative forcing (SARF) at the top of the atmosphere (TOA) and at the bottom of the atmosphere (BOA) was derived using the method shown in [3].

## 1. INTRODUCTION

Combined Raman lidar and Sun photometer measurements were conducted in Xinken and Beijing, China, in October 2004 and January 2005, respectively. Both measurement sites are located in highly industrialized and densely populated parts of the People's Republic of China. In China, the high rate of urbanization and economical growth is accompanied by increasing pollution of the environment. Uncontrolled emission of aerosols is a major problem for the whole region [4], leading to increased optical depth in the past 30 years [5]. Unlike aerosols from countries in Europe and North America the Chinese aerosols contain a much higher amount of strongly absorbing black carbon [6]. Main types of aerosols are dust (road dust as well as desert dust, esp. for Beijing), industry and traffic emissions and products from the combustion of biomass and fossil fuel. As detailed observations of Chinese aerosols are limited [6], widespread investigations need to be performed for a realistic estimation of the climatic impact of present and future aerosol pollution in eastern Asia.

## 2. MEASUREMENTS AND DATA PROCESSING

Aerosol optical properties, the vertical extent of the haze layer, and the vertical mixing of particles within the haze layer were analyzed with Raman lidar and Sun photometer. The portable Raman lidar system (POLLY) [7] enables us to measure the volume extinction and backscatter coefficients ( $\alpha$  and  $\beta$ , respectively), and thus the extinction-to-backscatter ratio (or lidar ratio)  $S$  at a wavelength of 532 nm. During daytime, when Raman signals cannot be detected, the lidar provides profiles of the backscatter coefficient only. As pointed out in [8], the relative errors of the lidar-derived aerosol data are mainly determined by signal noise and do not exceed 5%. Nighttime extinction profiles and daytime backscatter profiles were restricted to a minimum height of 350 m because of the overlap effect. During nighttime, the ratio of elastic to Raman-scattered signals was used for the determination of the backscatter coefficient down to 60-m height.

The SPM measures particle optical depth  $\tau_p$  at 8 wavelengths between 380 and 1044 nm with a temporal resolution of 30 s during daytime. The instrument was calibrated by intercomparison with the Leipzig AERONET Sun photometer. Uncertainties in optical depth are of the order of 0.015 (for 402-1044 nm) and 0.03 (for 380 nm) around noon and about a factor of 2 less at lower Sun elevations. The lidar measurements were used for cloud screening.

## 3. INVERSION PROCEDURE

The optical data from lidar and Sun photometer were used as combined input for an inversion algorithm [2] that has originally been designed for the inversion of multi-wavelength Raman lidar data. Simulations regarding the adaptability of the inversion to a combination of lidar/Sun photometer measurements are described in [1]. The combination of backscatter and extinction coefficients is needed in order to produce not only estimates on particle effective radius

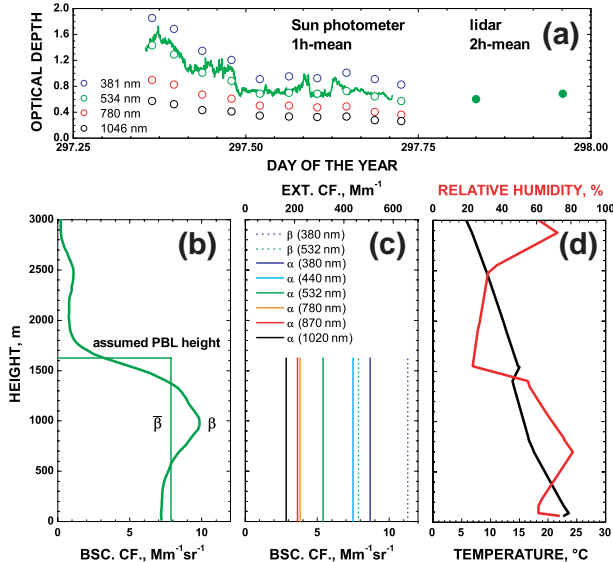


Fig. 1. Xinken, October 23, 2004; (a):  $\tau_p$  derived from SPM (open circles) and lidar measurements (closed circles); (b): profile of the backscatter coefficient  $\beta$  and the PBL-mean  $\bar{\beta}$ ; (c): created dataset of  $2 \times \beta$  and  $6 \times \alpha$  to run the inversion algorithm; (d): radio sounding of temperature and relative humidity. Radiosonde was launched at King’s Park, City University of Hong Kong.

and integral values of the particle size distribution, but also estimates on the single-scattering albedo. In that respect simulations have shown that particle backscatter coefficients measured at two wavelengths are needed for a reliable retrieval of the single-scattering albedo. The POLLY system measures particle backscattering at one wavelength only. Thus one of the tasks in data processing consisted of generating the missing backscatter information. Fig. 1 serves as an example for the following description of data pre-processing. The time lag between the measurements of lidar and SPM should be as short as possible associated with a low difference in optical depth (Fig. 1 (a):  $\Delta t < 3\text{h}$ ,  $\Delta\tau_p < 0.03$ ). If the PBL shows a well-mixed state (can be evaluated by use of radio soundings as shown in Fig. 1 (d):  $h \approx 1.6\text{ km}$ ) and the  $\beta$ -profile varies slightly with height, a PBL-mean backscatter coefficient can be assumed to be representative for the condition in the PBL (Fig. 1 (b):  $\bar{\beta} = 8\text{ Mm}^{-1}$ ). Knowledge of the PBL height permits the determination of PBL-mean extinction coefficients from optical depths (=height-integrated extinction coefficient). Optical depths at 381 and 532 nm were used to derive the Ångström exponent of the extinction  $\hat{a}_\alpha$ . Under the assumption  $\hat{a}_\alpha = \hat{a}_\beta$ , the backscatter coefficient at 381 nm wavelength could be acquired from the lidar-derived  $\beta(532\text{ nm})$ .

Two sets of input data were generated. One set con-

sists of extinction data ( $6 \times \alpha$ ) only and another consists of a combination of  $2 \times \beta$  and  $6 \times \alpha$ . Eleven inversion runs were carried out for each set of optical data. The mean values of the optical data were used in one inversion run. For the 10 remaining runs a distortion of 10% was applied to the input dataset. The mean value and the standard deviation of the parameters from the 11 runs were used as the inversion result. To estimate the error in the determination of  $\beta(381\text{ nm})$  the whole procedure was repeated with a systematic deviation of  $\pm 20\%$  of  $\beta(381\text{ nm})$ . Thus, for every inversion case we made 33 individual inversion runs.

#### 4. RESULTS AND DISCUSSION

Very different aerosol conditions were found during the two measurement campaigns: subtropical summer conditions with a high aerosol load and a well-mixed haze layer up to heights of 3 km in Xinken, and mid-latitude winter conditions with very clean and dry air and limited boundary-layer activity in Beijing. An overview of the results of the aerosol optical properties of the Xinken campaign is given in [8]. In Xinken the particle optical depth (at  $\lambda \approx 532\text{ nm}$ ) ranged from 0.21–1.77 with an average of  $0.94 \pm 0.33$ . Ångström exponents varied from 0.61–1.34 (mean:  $0.97 \pm 0.16$ ) and from 0.69–1.55 (mean:  $1.20 \pm 0.15$ ) for the wavelengthrange from 380–502 nm and from 502–1044 nm, respectively. The extinction-to-backscatter ratio ranged from 35–59 sr (mean:  $47 \pm 6\text{ sr}$ ). A mean PBL height of  $2.1 \pm 0.5\text{ km}$  was observed with individual values ranging from 0.9–3.2 km.

The inversion based on pure extinction data (run with the  $6 \times \alpha$  dataset) produces reliable results of the surface-area concentration  $s$  and the volume concentration  $v$ , and thus of the effective radius  $r_{\text{eff}}$  of the particles. Adding lidar-derived backscatter informa-

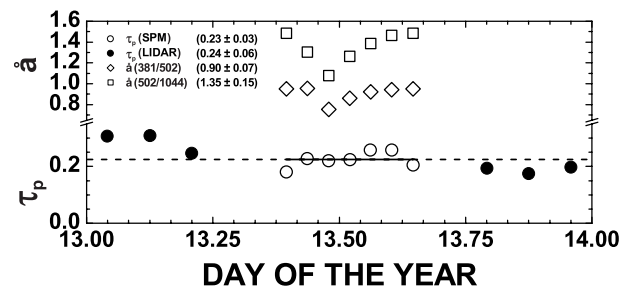


Fig. 2. Aerosol optical depth  $\tau_p$  measured with Sun photometer (1h-means, 534 nm, open circles) and Raman lidar (2h-means, 532 nm, closed circles) on January 13, 2005 in Beijing. Ångström exponents  $\hat{a}$  (diamonds for 381–502 nm, squares for 502–1044 nm) are derived from daytime SPM measurements.

Tab. 1. Comparison of the inversion-derived aerosol microphysical properties with in-situ based model results.

	Xinken		in-situ	Beijing	
	Inversion			Inversion	
	$2\beta + 6\alpha$	$6\alpha$		$2\beta + 6\alpha$	$6\alpha$
$r_{\text{eff}} [\mu\text{m}]$	$0.24 \pm 0.07$	$0.23 \pm 0.04$	$0.24 \pm 0.01$	$0.23 \pm 0.06$	$0.24 \pm 0.04$
$v [\mu\text{m}^3/\text{cm}^3]$	$80 \pm 20$	$70 \pm 20$	$90 \pm 10$	$25 \pm 7$	$27 \pm 6$
$a [\mu\text{m}^2/\text{cm}^3]$	$1000 \pm 200$	$1000 \pm 100$	$1200 \pm 100$	$330 \pm 60$	$330 \pm 40$
$n [\text{cm}^{-3}]$	$4900 \pm 2600$	$4500 \pm 1900$	–	$1700 \pm 700$	$1300 \pm 300$
$m_{\text{real}}$	$1.57 \pm 0.11$	$1.60 \pm 0.13$	–	$1.62 \pm 0.11$	$1.42 \pm 0.10$
$m_{\text{imag}}$	$0.02 \pm 0.02$	$0.02 \pm 0.01$	–	$0.02 \pm 0.01$	$0.01 \pm 0.01$
$\omega(532 \text{ nm})$	$0.77 \pm 0.12$	–	0.84	$0.78 \pm 0.11$	–

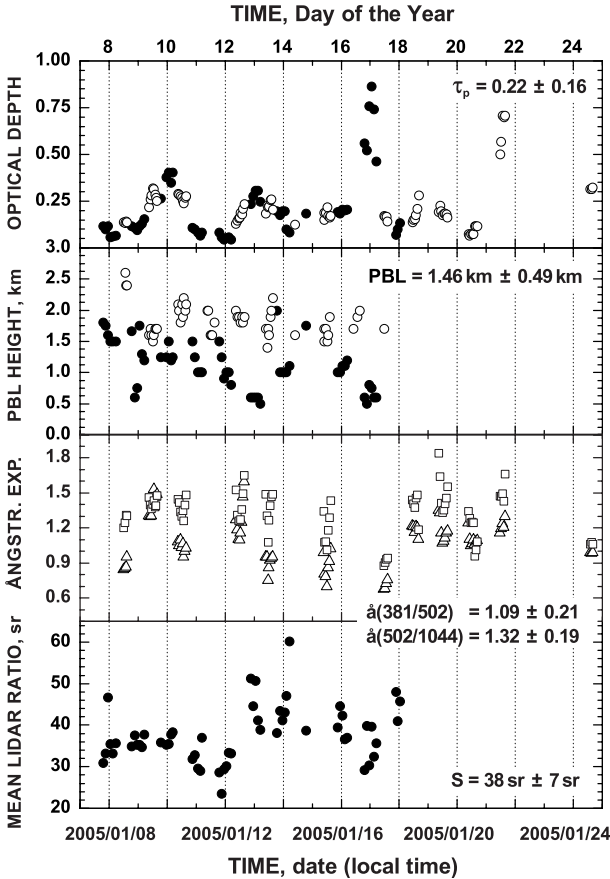


Fig. 3. Cloud-screened daytime (open symbols) and nighttime observations (closed symbols) of  $\tau_p(532\text{--}534 \text{ nm})$ , PBL height,  $\hat{a}$  (triangles for 381–502 nm, squares for 502–1044 nm), and column averaged lidar ratio  $S(532 \text{ nm})$ . 1-hour (daytime) and 2-hour mean values (nighttime) are shown. Numbers indicate mean values and standard deviations.

tion enables the determination of the complex refractive index, and thus of the single-scattering albedo  $\omega$ .

For the Xinken campaign an intercomparison with simultaneously conducted in-situ measurements and resulting Mie-model calculations [9] could be performed to validate the inversion results. As shown

in Tab. 1 a good agreement between in-situ and inversion-derived results is found. One should keep in mind that in-situ and column-integrated results are compared.  $r_{\text{eff}}$  and  $\omega(532 \text{ nm})$  are between 0.22 and 0.28  $\mu\text{m}$  (mean:  $0.24 \pm 0.07 \mu\text{m}$ ) and 0.73 and 0.82 (mean:  $0.77 \pm 0.12$ ), respectively, for the Xinken site. Fig. 2 shows a comparison of the lidar- and Sun-photometer-derived total particle optical depth for a typical measurement day in Beijing (January 13, 2005; Day of the Year (DOY) 13). The Ångström exponents, which describe the wavelength dependence of  $\tau_p$ , decrease with increasing particle size. The numbers shown in Fig. 2 indicate comparably large particles. Fig. 3 gives an overview of the particle optical properties and PBL heights derived from the January measurements at Beijing. Particle optical depth was much lower than at Xinken. Values between 0.04 and 0.87 with an average value of  $0.21 \pm 0.19$  were observed. Most results (66%) were found in the range between 0.1 and 0.3. The Sun photometer derived Ångström exponents were between 0.67 and 1.59 and 0.88 and 1.84 with mean values of 1.09 and 1.32 for wavelengths from 380–502 nm and from 502–1044 nm, respectively. Lidar ratios varied from 24–60 sr with a mean value of  $38 \pm 7 \text{ sr}$ . The PBL did not exceed heights of 2.6 km. On average it extended up to  $1.5 \pm 0.5 \text{ km}$ . The results of the inversion of the optical data are similar to the findings for Xinken.  $\omega$  varied from 0.74–0.82 (mean:  $0.78 \pm 0.11$ ). Effective radii were between 0.22 and 0.29  $\mu\text{m}$  (mean:  $0.23 \pm 0.06 \mu\text{m}$ ).

In Xinken several days of pronounced boundary-layer development were observed. As described in [10], the high aerosol load affects the development of the PBL. As sunlight is absorbed by the particles, the column of air warms up, thus leading to a stabilization of the layering. Hence, convective mixing is blocked which in turn leads to lower PBL heights. Two selected days are shown in Fig. 4, covering the time period from October 23 to 24, 2004 (DOY 297.0–299.0, local time (lt)). The time- and height-resolved background- and height-corrected signal,

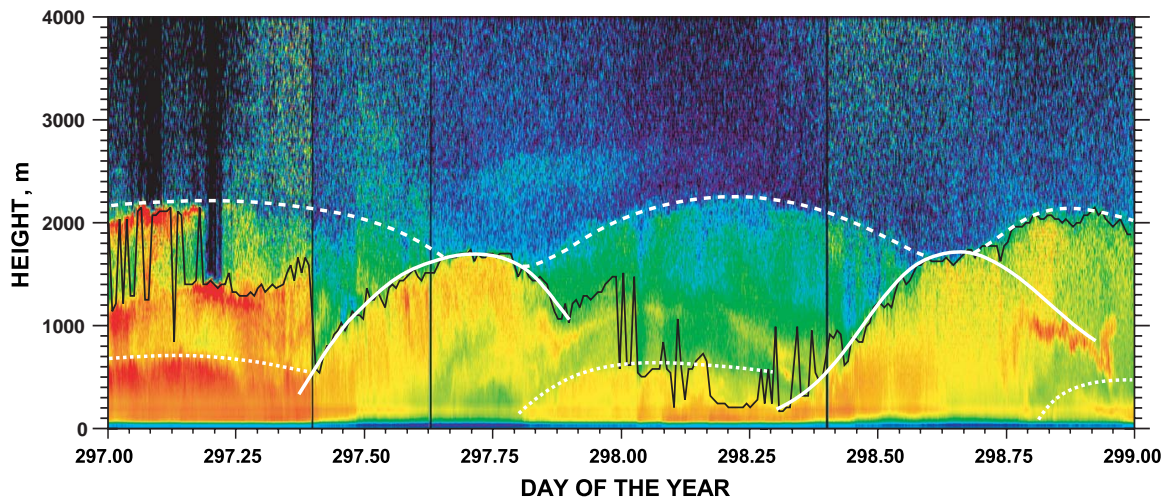


Fig. 4. Development of the planetary boundary layer at Xinken, China, from October 23, 00:00 Lt, to October 25, 00:00 Lt (DOY 297.0–299.0 2004). The height- and transmission-corrected signal is shown. The explanation is given in the text.

an automatically retrieved PBL height (black line) [11] and subjectively (by eye) estimated PBL heights (white lines) are shown. In the automatic algorithm the range of the strongest gradient in the received signal is defined as top of the PBL. The observer used the color coding to identify the top of the PBL. With sunrise the planetary boundary layer started to develop (solid white line), leading to a final height of about 2 km in the afternoon. After sunset, the PBL collapsed and a nocturnal boundary layer (dotted white line), with a remaining haze/residual layer on top (dashed white line), started to develop.

Furthermore, solar aerosol radiative forcing (SARF) was estimated by means of the column integrated backscatter coefficient  $\beta_c = \tau_p/S$  for both campaigns. For the Xinken measurements, SARF was on average  $-83 \pm 36 \text{ W/m}^2$  at the TOA and  $-173 \pm 75 \text{ W/m}^2$  at the BOA with maximum values of  $-164 \text{ W/m}^2$  and  $-345 \text{ W/m}^2$  at TOA and BOA, respectively. These results are in agreement with maximum values of  $-250 \text{ W/m}^2$  derived by radiative transfer calculations [10]. SARF was found to be  $-32 \pm 17 \text{ W/m}^2$  and  $-51 \pm 30 \text{ W/m}^2$  at the TOA and at the BOA, respectively, over Beijing.

## REFERENCES

1. Pahlow M., et al., Retrieval of aerosol properties from combined multiwavelength lidar and sun photometer measurements: simulations, *Appl. Opt.*, submitted, 2006.
2. Müller D., et al., Microphysical particle parameters from extinction and backscatter lidar data by inversion with regularization: simulation, *Appl. Opt.*, 38, 2346–2357, 1999.
3. Wendisch M., et al., Potential of lidar backscatter data to estimate solar aerosol radiative forcing, *Appl. Opt.*, 45, 770–783, 2006.
4. Streets B. G., et al., An inventory of gaseous and primary aerosol emissions in Asia in the year 2000, *J. Geophys. Res.*, 108, 2002JD003093, 2003.
5. Luo Y., et al., Characteristics of the spatial distribution and yearly variation of aerosol optical depth over China in last 30 years, *J. Geophys. Res.*, 106, 2001JD900030, 2001.
6. Huebert B. J., et al., An overview of ACE-Asia: Strategies for quantifying the relationships between Asian aerosols and their climatic impacts, *J. Geophys. Res.*, Vol. 108, 2003JD003550, 2003.
7. Althausen D., et al., Portable Raman lidar for determination of particle backscatter and extinction coefficients, *Reviewed and Revised Papers Presented at the 22nd ILRC, Matera, Italy*, 83–86, 2004.
8. Ansmann A., et al., High aerosol load over the Pearl River Delta, China, observed with Raman lidar and Sun photometer, *Geophys. Res. Letts.*, 32, 2005GL023094, 2005.
9. Cheng Y.-F., et al., The mixing state of black carbon and non-absorbing aerosol components derived from in situ particle optical properties at Xinken in Pearl River Delta of China, *J. Geophys. Res.*, submitted, 2005.
10. Heintzenberg J., et al., Light absorbing particles reduce air ventilation over the Pearl River Delta, China, *Nature*, in review, 2006.
11. Brooks I. M., Finding boundary layer top: Application of a wavelet covariance transform to lidar backscatter profiles, *J. Atmos. Oceanic Technol.*, 20, 1092–1105, 2003.